High aspect ratio GaN fin microstructures with non-polar sidewalls by continuous mode MOVPE

Jana Hartmann,[1,2], Frederik Steib[1,2], Hao Zhou[1], Johannes Ledig[1,2], Sönke Fündling[1,2], Friederike Albrecht[1,2], Tilman Schimpke[3], Adrian Avramescu[3], Tansen Varghese[3], Hergo-Heinrich Wehmann[1,2], Martin Straßburg[3], Hans-Jürgen Lugauer[3], Andreas Waag[1,2]*

[1]Institut für Halbleitertechnik and Laboratory for Emerging Nanometrology, Technische Universität Braunschweig, 38092 Braunschweig, Germany

[2] epitaxy competence center ec[2], Hans-Sommer-Strasse 66, 38106 Braunschweig, Germany

[3]Osram Opto Semiconductors GmbH, Leibnizstraße 4, 93055 Regensburg, Germany

*Corresponding author: Jana.Hartmann@tu-bs.de

KEYWORDS GaN fins, GaN nanowalls, GaN nanosheets, GaN lamella, high aspect ratio non-polar a-plane GaN surfaces, 3D GaN

ABSTRACT Three-dimensional GaN micro- and nanorods with high aspect ratio have recently gained substantial interest in LED research, due to their reduced defect density, their non-polar sidewalls and their increased active area. Here, we present an alternative geometry for high aspect ratio 3D nanostructures: vertically standing GaN “walls”, so called GaN fins. With high aspect ratios, these GaN fins exhibit the same interesting characteristics as their rod counterparts mentioned above. Beyond that, due to their geometry, the respective material analysis and device

https://doi.org/10.24355/dbbs.084-201912181044-0

processing can be expected to be less complex. We are able to demonstrate the highly reproducible selective area growth of these fins by continuous mode MOVPE. Fin heights of more than 50 µm (aspect ratios of nearly 14) could be achieved and growth rates are as high as 22.8 µm/h in the beginning of the growth. The sidewalls are smooth non-polar <11-20> a-planes, suitable for optoelectronic devices due to the missing quantum-confined Stark effect and less edge effects compared to rods. We investigate the influence of pattern orientation and geometry on the fin morphology. Moreover, the influence of silane flow, which is known to enhance the vertical growth rate, and other growth parameters are systematically explored.

INTRODUCTION GaN is the material of choice for solid state lighting since many years. Conventional light emitting diodes (LEDs) based on the (Al,In,Ga)N material system are generally grown in a planar geometry using c-oriented thin film deposition. These planar GaN, AlGaN and InGaN films are characterized by a huge density of threading dislocations due to lattice mismatch to each other and to the underlying growth substrate, typically sapphire, SiC or silicon. The polar c-orientation of the layers leads to high piezoelectric fields in the multi quantum well (MQW) region. In spite of these properties, very high quantum efficiencies can be reached in LEDs for certain indium concentrations, but both high defect density and piezoelectric effects are viewed as being disadvantageous for certain applications like laser diodes or higher indium content quantum wells. The m-plane quantum wells of three-dimensional (3D) micro- or nanorods in a core-shell geometry are both defect free and free of piezoelectric effects[1]. In addition, the large sidewall surface allows for increasing the light emitting area of LED devices without increasing the necessary substrate area[2], potentially reducing production cost per lumen substantially and increasing the luminous density.

https://doi.org/10.24355/dbbs.084-201912181044-0

Three-dimensional (3D) GaN structures are usually either directly grown by MOVPE in a selective area growth (SAG) process in order to reduce the dislocation density due to the small footprint[3], or deep etched into a GaN thin film in order to release its strain[4]. 3D n-GaN structures have already been used as the basis for core-shell LEDs with MQW and p-GaN shell layers[5]. These QWs do not exhibit the quantum-confined Stark effect (QCSE)[6], since they are grown on non-polar m-oriented sidewalls.

As already mentioned in literature, there are several advantages of core-shell rod LEDs over conventional planar LEDs[7,8]. In order to exploit these interesting advantages, the 3D geometry does not necessarily need to be rod-like, but could also be in a so-called fin shape, including a few distinct advantages in comparison to microrod structures. These fin structures are long, thin and high GaN walls with non-polar sidewalls and aspect ratios (height to width as well as length to height) much larger than one. The growth of III-nitrides in fine wall-shaped structures, mainly by molecular beam epitaxy (MBE), was already shown by Kishino and Kikuchi[9]. MOVPE growth of these fin structures was demonstrated by T.-W. Yeh et al.[10] and by A. K. Rishinaramangalam et al[11]. Due to the small footprint of fins and due to defect annihilation at the sidewall surfaces, lower defect densities can be expected as compared to planar GaN layers. In addition, core-shell fin LEDs have, under certain circumstances, an even larger active area ratio (AAR), i.e. active area (equivalent to surface area) to substrate area in comparison with core-shell rod LEDs: For hexagonally shaped rod LEDs in a hexagonal pattern $AAR_{rod} = \frac{6}{\sqrt{3}}\frac{H*D}{P^2}$ with considering the height H, diameter D (defined as two times the circumradius of the hexagonal rod) and pitch P (defined as distance between the centers of neighboring structures) of the columns, respectively. If the end facets of the fins are neglected, for fin LEDs it is $AAR_{fin} = \frac{2H}{P}$ with the height H and pitch P of the fins, respectively. Taking the same diameter D (for rods) or width W (for fins) and

https://doi.org/10.24355/dbbs.084-201912181044-0

the same height and pitch for rods and fins, there is an enhancement in the AAR of $\frac{AAR_{Fin}}{AAR_{rods}} = \frac{P}{\sqrt{3}D}$. For a pitch of more than 1.7 times the diameter or width, the AAR for fins is larger than that for rods. This prerequisite is fulfilled in most core-shell rod LED designs, since the outer shell layers, e.g. the p-GaN, need additional space in between the structures. Furthermore, the structures should have enough distance between each other to couple out light with high efficiency. If micro-grained optical converter materials filled into the 3D-ensemble are used for white light applications, even more space is required between the rods or fins.

Besides the greater AAR of fins, the vertical current density in the fin LED core is less than in a rod core, assuming comparable active area and driving conditions. This is due to a larger footprint area per active area for fins than for rods. Thus, the current density in the base area is reduced and less problems regarding heating can be expected in fin LEDs. For rod LEDs the footprint ratio $FR_{rod} = \frac{\sqrt{3}D}{8H}$, while for fin LEDs it holds $FR_{fin} = \frac{W}{2H}$. Taking again the same diameter or width and the same height for rods and fins, there is an enhancement of $\frac{FR_{fin}}{FR_{rod}} = \frac{4}{\sqrt{3}} \approx 2.31$.

Another advantage of GaN fins is their much easier fabrication: Less effort is needed for lithography masks since a precise pattern profile is necessary in one dimension only, which is less critical for nanoimprint lithography and allowing laser interference methods to be used. Also, the analysis of single fin LEDs is much easier. E.g. by cleaving the samples perpendicular to the fin longitudinal direction, a cross-sectional view into the structures can easily be achieved, which is extremely difficult for rod geometries. Also, GaN fins have higher mechanical stability than rods and therefore are less sensitive to further processing steps. Unlike GaN fins, rod structures offer six large edge lines between the sidewall facets. Therefore, boundary effects, like e.g. an increased indium content at the edges between two non-polar planes due to different strain relaxation[12,13]

https://doi.org/10.24355/dbbs.084-201912181044-0

could become an issue. In this respect, fins can be expected to be much more homogeneous. For the same reason, the current conducting path inside the n-GaN core could be more uniformly for GaN fins[10]. Last but not least, the fins provide relatively large non-polar surfaces, each of several thousand μm², at a low cost. These surfaces could be viewed as "vertical a-plane GaN pseudo substrate" with low defect density, which can be used to study the properties of non-polar GaN without the necessity to use very expensive a-oriented GaN substrates. Such fins could be applied for LEDs[10,11], but also for laser structures, Fin-FETs or HEMTs, waveguides[14] and much more.

GaN fins, also called nanowalls or nanosheets in other publications, with {1-100} non-polar sidewall planes and aspect ratios of two or more have already been fabricated by pulsed growth mode selective area in MOVPE[10,11]. In this article, we demonstrate the growth of GaN fins with {11-20} non-polar sidewalls by continuous growth mode selective area MOVPE. The growth rates are enhanced compared to pulsed growth mode and thus large vertical dimensions of the fins are shown. Aspect ratios of almost 14 could be achieved, the highest ever reported for bottom-up GaN fin geometries. The dependencies on pattern orientation, pattern geometry and growth conditions are described.

EXPERIMENTAL SECTION The fin structures were grown by SAG on 2" wafer templates of two different kinds, either SiO_x on GaN on sapphire or SiO_x directly on sapphire. The 30 nm thick SiO_x masking layer was structured by photolithography. Either a lift-off process with an image reversal lithography step and SiO_x evaporation or a positive lithography step with subsequent dry etching of the SiO_x (by inductively coupled plasma, using SF_6) is applied. The photolithography is done with a 300 nm thick layer of AZ 5214E. Both techniques resulted in very comparable fin-like structures. The lithography mask consists of different patterns of line openings with lengths of 10 μm, 25 μm, 50 μm, 100 μm, 250 μm, 500 μm and 1000 μm, with pattern widths (W_p) of 0.5

https://doi.org/10.24355/dbbs.084-201912181044-0

µm, 1 µm, 1.5 µm and 2 µm and pitches of three, six and nine times the width (see Figure 1). These patterns are repeatedly rotated by 15° relative to each other, arranged in a circle with six patterns of lines parallel to the a-direction (resulting in fins with m-plane sidewalls), six patterns of lines parallel to the m-direction (resulting in fins with a-plane sidewalls) and additional twelve patterns oriented in directions in between these two. Besides of this main circle of patterns, at the rim of the photolithography mask are structures with even longer line openings and with smaller rotation angles relative to m- and a-direction. The orientation of the lines is given as the angle to the sapphire wafer flat, taking into account the 30° twist of GaN growth with regard to the sapphire crystal. The angular alignment of the photolithography mask with respect to the GaN crystal is crucial and was secured by optical alignment. After patterning of the SiO_x mask, the templates were cleaned in an O_2 plasma. A vertical close coupled showerhead reactor with a 3 x 2" susceptor is used. The SAG of fins is similar to the process used for growth of GaN rods[15,5]. In the case of a SiO_x on sapphire template, the growth process started with a nitridation, followed by a nucleation step and a 3D growth step with a V/III ratio of 150 at a temperature of 1070°C for 1500 s. The applied silane flow was 16.5 nmol/min. In the case of a SiO_x on GaN on sapphire template, the growth process started with a cleaning step at high temperature under H_2 atmosphere, followed by a filling step under layer growth conditions, standardly for 50 s, and a 3D growth step at 1060°C, a V/III ratio of 77 and a SiH_4 flow of 0 nmol/min, 16.5 nmol/min or 36 nmol/min. Besides the silane flow, the filling time as well as the time of the 3D growth step have been varied.

All data in this article were determined from scanning electron microscopy (SEM) images. The width of the fins, which is usually significantly larger than the pattern width W_p of the SiO_x mask, is called W_r ('real width') here. For all statistical analysis, both, the width W_r and the height of the fins H were measured at three different points in each of four different patterns which have a length

https://doi.org/10.24355/dbbs.084-201912181044-0

of 1000 µm and which have the same orientation of the lines. Only patterns with regular and homogenous growth were taken into account for the statistics.

All sidewall facets were characterized by measurements of their angle with respect to the c-plane in cross-sectional SEM images.

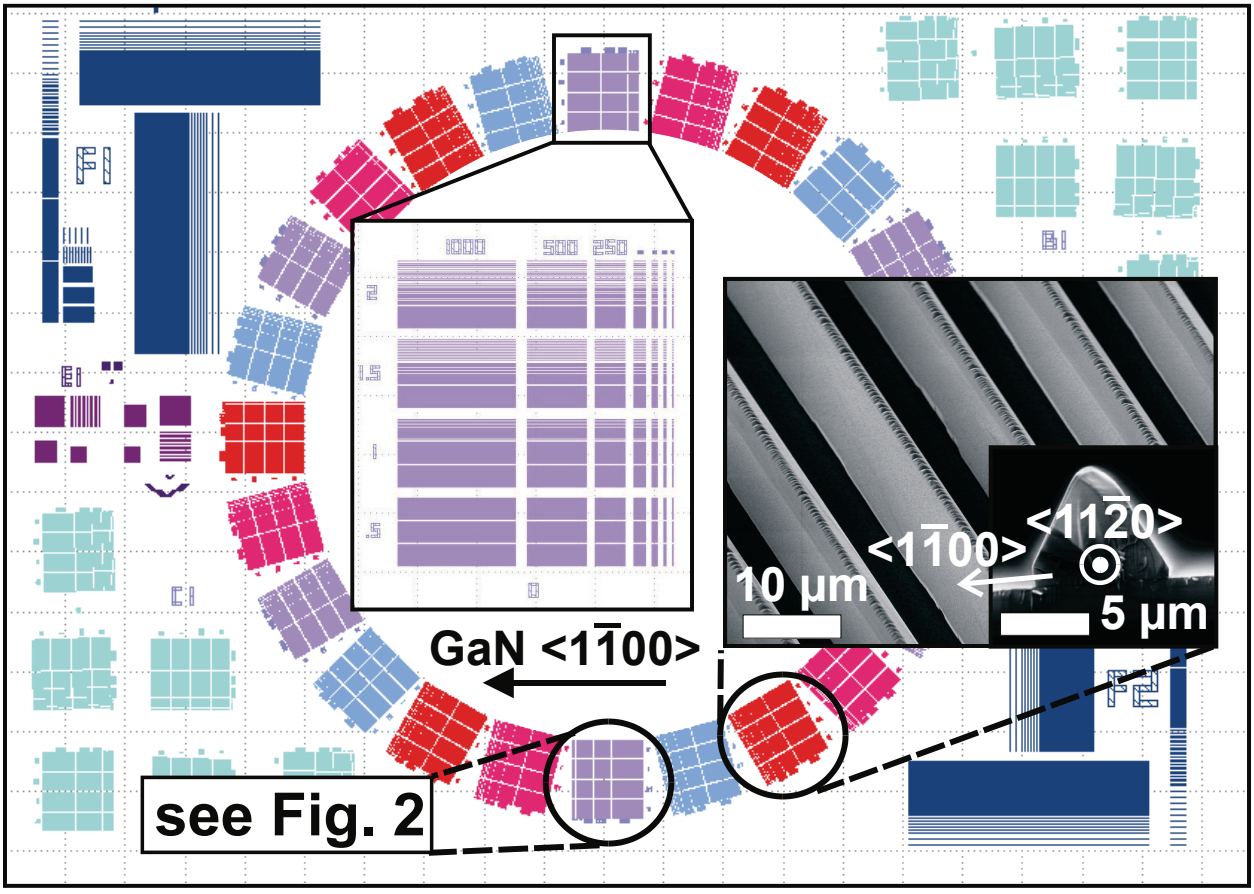

Figure 1. Photolithography mask design with 24 fields rotated by 15° to each other and with one field shown in higher magnification, the inset shows SEM images of m-plane fins

RESULTS AND DISCUSSION

First, the SAG on GaN on sapphire templates will be discussed. If the mask lines are parallel to the a-direction, fins with {1-100} m-plane sidewalls emerged (inset in Figure 1). We call these fins m-plane fins from now on. Besides the m-plane sidewalls, the polar (0001) and semipolar

https://doi.org/10.24355/dbbs.084-201912181044-0

(mostly {1-101}) planes occurred, as also reported in other publications[16,17]. The semipolar facets are dominating the GaN fin structures observed in our case (see SEM image of cross-section in Figure 1 inset). Reasons for the large semipolar facets could be the relatively slow growth rate of the semipolar facet[18,19] and the large mask line widths compared to the experiments by T.-W. Yeh et al.[17]. For high V/III ratios, similar results are published[18], especially for the use of large widths of the mask openings[20].

For lines oriented in the m-direction, high aspect ratio fin structures with {11-20} a-plane sidewalls and a top surface consisting of some small semipolar facets with different facet angles were formed (Figure 2). These fins will be called a-plane fins from now on. The non-polar sidewalls have very smooth surfaces, whereas the top surface appears with a higher roughness (Figure 2b). For the growth on c-plane GaN, Sun et al.[21] determined kinetic Wulff plots by differential SAG for two different GaN growth modes. For both of their growth conditions, the semipolar {11-22} facets showed a larger growth rate than the semipolar {10-11} facets[21]. Under specific growth conditions, the growth rate of {11-22} is even four times higher than that of {10-11}, as shown by Aagesen et al.[19]. For convex geometries like in the case of fin growth, the SAG structure is determined by the facet with lowest growth rate. Therefore, typically the {10-11} facets emerge more pronounced than the {11-22}. This could explain the structural differences observed in these GaN m-plane and a-plane fins. Henceforth, all further analysis is based on a-plane fins.

In our case, the enlargement of the fin width W_r with respect to the pattern width W_p was not due to a misalignment as described elsewhere[10], since an intended misorientation of 2° led to thinner or comparable W_r in our experiments. However, along the sidewalls of these intentionally misoriented lines, we found lots of steps, i.e. segments of m-facets (up to 1 µm in length) within the otherwise a-plane sidewalls. They appear in a mean distance of 6.25 µm, whereas on standard

https://doi.org/10.24355/dbbs.084-201912181044-0

patterns oriented precisely along the m-direction, we found the period of steps increased to 20 µm accompanied by a reduced length of below 200 nm. Therefore, we assume that the precision of the angular alignment during the photolithography is good enough to avoid uncontrolled influence of unintentional misalignments.

At the rim along the line openings in the SiO_x mask, a deep etching of the underlying GaN buffer can be observed (Figure 2c). As concluded from growth experiments, this etching is occurring during the high temperature cleaning step under H_2 atmosphere at the beginning of the growth process. Some fins show vertically oriented holes, sometimes penetrating through their center from bottom to top, as it can be seen in the leftmost fin in Figure 2c. These holes are probably forming because there is no full coalescence of the initially separate seeds which nucleate in the mask openings starting from the rims.

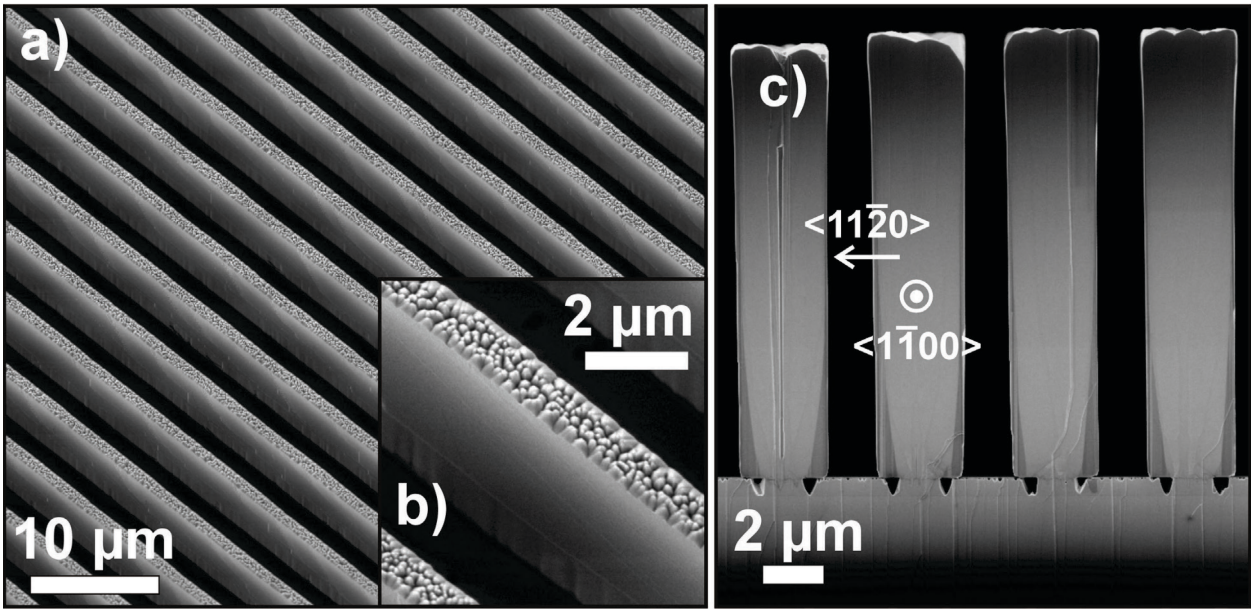

Figure 2. (a) SEM overview (5 kV, 40° tilt) of GaN a-plane fin pattern grown with 36 nmol/min SiH_4 for 1200 s and (b) higher magnification of the same pattern, (c) cross sectional SEM image (2 kV, 90° tilt) for GaN fins grown with 16.5 nmol/min SiH_4 for 2400 s

https://doi.org/10.24355/dbbs.084-201912181044-0

The growth of a-plane fins is strongly dependent on the pattern geometry (pitch/width). In general, for larger widths (W_p) and smaller pitches of the lines in the mask a more regular growth was achieved, i.e. the fins are homogenous in width and height along their length and they are very similar to their neighbouring fins in the same and corresponding patterns. Hence, the most comparable fins were grown in the patterns W1.5 P4.5 (width of 1.5 µm and pitch of 4.5 µm), W2 P6 and W2 P12. We achieved growth of GaN fins both directly on sapphire substrates and on GaN buffer layers on sapphire. As expected, the dependence of the fin structure on the line orientation is the same in both cases. However, comparing the fins on these two different templates, the fins grown on the GaN buffer layer (growth time of 1200 s, 16.5 nmol/min SiH_4) reach larger heights, e.g. in pattern W1.5 P4.5 they are 8.3 ± 0.6 µm, compared to fins grown on sapphire (growth time of 1500 s, 16.5 nmol/min SiH_4) which reach a height of 4.0 ± 0.4 µm in the same pattern. Possible explanations for this height disparity could be either a growth delay on the sapphire template or an influence of the varying V/III ratio used on the different templates. The width of the fins is the same in both cases, and thus the aspect ratio is increasing for fins grown on GaN buffer layers. For waveguide applications the growth directly on sapphire could be advantageous. For core-shell fin LEDs, fins on a GaN buffer layer are superior because of the electrical contact of all structures via the n-doped buffer layer. Therefore and due to the higher aspect ratios, in the following sections fins grown on SiO_2/GaN/sapphire templates will be discussed in more detail.

In order to examine the growth parameters for fin growth, the filling time, i.e. the duration of the first growth step under layer growth conditions, was varied from 0 to 150 s, followed by a 3D growth step of 1200 s duration. For 0 s filling time, fins evolved but their height was reduced by ca. 40 % in comparison to longer filling times. In most of the patterns, the largest heights were achieved with a filling time of 50 s. This seems to be the optimum duration for enough but not too

https://doi.org/10.24355/dbbs.084-201912181044-0

many nucleation points. In the following, we studied the fins in more detail for a constant filling time of 50 s.

By comparing fins grown for 1200 s with and without silane, the height of the fins grown with 16.5 nmol/min SiH_4 increased by about two times as expected due to a larger vertical growth rate by using SiH_4[22,5,23,24]. Nevertheless, also silane-free growth was possible and heights of 8.6 ± 0.5 µm (pattern W2 P12) were reached. For the pattern W1.5 P4.5 the fins were 4.17 ± 0.26 µm high which corresponds to a growth rate of 12.5 µm/h without silane.

To investigate the growth rate evolution over the time, the duration of the 3D growth step was varied from 600 s to 3 h, with a constant filling time of 50 s and a SiH_4 flow of 16.5 nmol/min. In Figure 3 the height and the width of the fins are plotted.

https://doi.org/10.24355/dbbs.084-201912181044-0

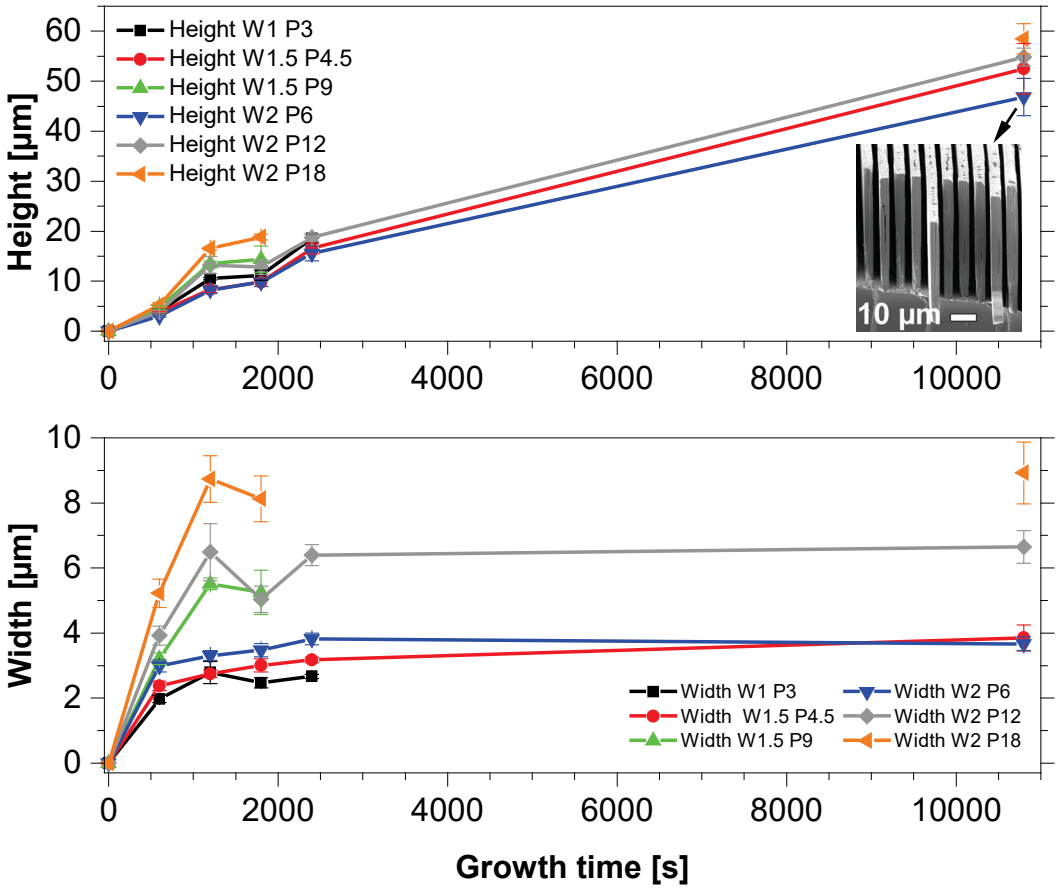

Figure 3. Measured height and width of a-plane fins with varying mask-opening width/µm (W) and pitch/µm (P) plotted over the growth time (each growth time corresponds to an individual sample). Inset shows a cross section of high aspect ratio fins grown for 10800 s. Some fins jut out over the cleaving edge of the sample.

Whereas the width stays roughly constant after more than 1200 s of growth duration, the height is increasing mostly linearly with growth time, as expected. The very high initial growth rates are decreasing to still high values for longer durations: The initial growth rate up to 600 s for pattern W1.5 P4.5 is as high as 22.8 µm/h. After 2400 s, the growth rate decreases to about 15.4 µm/h in the same pattern. The reason for this decrease of growth rate could be due to the vanishing contribution of the sidewall diffused species and therefore less material transport to the top facets, as already reported for GaN columns[25]. Nevertheless, the total growth rate of 17.5 µm/h (SiH_4

https://doi.org/10.24355/dbbs.084-201912181044-0

flow of 16.5 nmol/min) is much faster than the corresponding layer growth rates. For GaN rod growth, such high growth rates over long growth durations could be achieved only by adding a very high amount of silane (> 110 nmol/min)[25]. Summarizing, the new fin structures show significant higher vertical growth rates at low SiH_4 flows than the GaN rods. This fact is expected to be a substantial advantage of the GaN fin approach, since lower SiH_4 flows very likely lead to less point defects and therefore higher material quality. Furthermore the doping level can be controlled much better.

It is interesting to note that there is no length limitation (in the longitudinal direction) of the GaN fin structures observed until now. The longest fin with a continuous height (around 17 µm) that we could observe was 8 mm in length (with a width of 8 µm). It was only restricted by the maximum line length in the photolithography mask.

CONCLUSIONS For the first time continuous MOVPE growth mode has been used for fabricating GaN fins. High aspect ratios of up to 14 were achieved regarding height to width. The MOVPE growth of GaN fins with m- and a-plane sidewalls was studied systematically as a function of fin orientation and growth parameters. In contrast to other publications, in m-plane fins only low m-plane sidewalls evolve and the structures are dominated by semipolar facets. Though, in a-plane fins, high aspect ratio fins with smooth a-plane sidewalls emerge, being well suited for further development of light emitting devices. These a-plane fins were analyzed in more detail. The growth on masked sapphire templates was comparable to the growth on masked GaN on sapphire templates. The SAG is successful even without SiH_4 flow. High growth rates of up to 22.8 µm/h (with relatively low SiH_4 flow) were achieved in some patterns. Fins with heights of more than 50 µm were demonstrated for growth times of 10800 s. By increasing the time of the second 3D growth step, the width of the fins stayed almost constant, and the height was increasing linearly

https://doi.org/10.24355/dbbs.084-201912181044-0

with time without any indication of height saturation. GaN fins have many potential advantages over GaN rods, e.g. easier processing and growth, higher active area ratio (if the pitch is larger than 1.7 times the width/diameter) and larger non-polar facets without edge effects. GaN fin structures hence are suggested to be a very interesting new route for potentially realizing 3D light emitting devices for solid state lighting.

Corresponding Author

*** Electronic mail: Jana.Hartmann@tu-bs.de**

Funding Sources

DFG FOR1616, China Scholarship Council

ACKNOWLEDGMENT We thank the DFG (Research Unit FOR 1616: "Dynamics and Interactions of Semiconductor Nanowires for Optoelectronics") for financial support and the China Scholarship Council for scholarship support. We acknowledge Prof. M. Schilling for giving us the possibility to use his FESEM. Finally, we thank Juliane Arens for technical support.

ABBREVIATIONS

3D, QCSE, MOVPE, SAG, FF, QW, MQW, LED, FET, HEMT, FR, SEM

REFERENCES

(1) Mandl, M.; Wang, X.; Schimpke, T.; Kölper, C.; Binder, M.; Ledig, J.; Waag, A.; Kong, X.; Trampert, A.; Bertram, F.; Christen, J.; Barbagini, F.; Calleja, E.; Strassburg, M. *Phys. status solidi - Rapid Res. Lett.* **2013**, *7* (10), 800–814.

(2) Li, S.; Waag, A. *J. Appl. Phys.* **2012**, *111* (7), 071101.

(3) Hersee, S. D.; Sun, X.; Wang, X. **2006**, *221*.

(4) Shields, P.; Hugues, M.; Zúñiga-Pérez, J.; Cooke, M.; Dineen, M.; Wang, W.; Causa, F.; Allsopp, D. *Phys. Status Solidi Curr. Top. Solid State Phys.* **2012**, *9* (3-4), 631–634.

https://doi.org/10.24355/dbbs.084-201912181044-0

(5) Wang, X.; Li, S.; Mohajerani, M. S.; Ledig, J.; Wehmann, H.-H.; Mandl, M.; Strassburg, M.; Steegmüller, U.; Jahn, U.; Lähnemann, J.; Riechert, H.; Griffiths, I.; Cherns, D.; Waag, A. *Cryst. Growth Des.* **2013**.

(6) Koester, R.; Hwang, J. S.; Salomon, D.; Chen, X.; Bougerol, C.; Barnes, J. P.; Dang, D. L. S.; Rigutti, L.; De Luna Bugallo, A.; Jacopin, G.; Tchernycheva, M.; Durand, C.; Eymery, J. *Nano Lett.* **2011**, *11* (11), 4839–4845.

(7) Waag, A.; Wang, X.; Fündling, S.; Ledig, J.; Erenburg, M.; Neumann, R.; Al Suleiman, M.; Merzsch, S.; Wei, J.; Li, S.; Wehmann, H. H.; Bergbauer, W.; Straßburg, M.; Trampert, A.; Jahn, U.; Riechert, H. *Phys. Status Solidi Curr. Top. Solid State Phys.* **2011**, *8* (7-8), 2296–2301.

(8) Kang, M. S.; Lee, C.-H.; Park, J. B.; Yoo, H.; Yi, G.-C. *Nano Energy* **2012**, *1* (3), 391–400.

(9) Kishino, K.; Kikuchi, A. Group-III nitride structure and method for producing a group-III nitride structure, Patent US 2010/0252836 A1, 2010.

(10) Yeh, T. W.; Lin, Y. T.; Ahn, B.; Stewart, L. S.; Daniel Dapkus, P.; Nutt, S. R. *Appl. Phys. Lett.* **2012**, *100* (3), 033119.

(11) Rishinaramangalam, A.; Fairchild, M.; Ul Masabih, S.; Shima, D.; Balakrishnan, G.; Feezell, D. In *CLEO: 2014*; OSA: Washington, D.C., 2014; p SM2J.1.

(12) Lu, P. F.; Sun, C.; Cao, H. W.; Ye, H.; Zhong, X. X.; Yu, Z. Y.; Han, L. H.; Wang, S. M. *Solid State Commun.* **2014**, *178*, 1–6.

(13) Bi, Z.; Lindgren, D.; Johansson, B. J.; Ek, M.; Wallenberg, L. R.; Gustafsson, A.; Borgström, M. T.; Ohlsson, J.; Monemar, B.; Samuelson, L. *Phys. status solidi* **2014**, *11* (3-4), 421–424.

(14) Tanaka, T.; Uchida, K.; Watanabe, A.; Minagawa, S. *Appl. Phys. Lett.* **1995**, *976* (1996), 976.

(15) Wang, X.; Hartmann, J.; Mandl, M.; Sadat Mohajerani, M.; Wehmann, H.-H.; Strassburg, M.; Waag, A. *J. Appl. Phys.* **2014**, *115* (16), 163104.

(16) Shin, D. H.; Bae, M. K.; Yi, S. N.; Na, J. H.; Lee, K. H.; Taylor, R. A.; Doh, S. H.; Park, S. H. *Journal of the Korean Physical Society*. 2007, p 220.

(17) Yeh, T. W.; Lin, Y. T.; Ahn, B.; Stewart, L. S.; Daniel Dapkus, P.; Nutt, S. R. *Appl. Phys. Lett.* **2012**, *100* (3), 10–13.

(18) Kapolnek, D.; Keller, S.; Vetury, R.; Underwood, R. D.; Kozodoy, P.; Den Baars, S. P.; Mishra, U. K. *Appl. Phys. Lett.* **1997**, *71* (9), 1204.

(19) Aagesen, L. K.; Coltrin, M. E.; Han, J.; Thornton, K. *J. Appl. Phys.* **2015**, *117* (19), 194302.

(20) Kato, Y.; Kitamura, S.; Hiramatsu, K.; Sawaki, N. *J. Cryst. Growth* **1994**, *144* (3-4), 133–140.

(21) Sun, Q.; Yerino, C. D.; Leung, B.; Han, J.; Coltrin, M. E. *J. Appl. Phys.* **2011**, *110* (5), 053517.

(22) Haffouz, S.; Beaumont, B.; Gibart, P. *MRS Internet J. Nitride Semicond. Res.* **1998**, *30* (8),

https://doi.org/10.24355/dbbs.084-201912181044-0

e8.

(23) Koester, R.; Hwang, J. S.; Durand, C.; Dang, D. L. S.; Eymery, J. *Nanotechnology* **2010**, *21* (1), 015602.

(24) Tessarek, C.; Heilmann, M.; Butzen, E.; Haab, a.; Hardtdegen, H.; Dieker, C.; Spiecker, E.; Christiansen, S. *Cryst. Growth Des.* **2014**, *14* (3), 1486–1492.

(25) Hartmann, J.; Wang, X.; Schuhmann, H.; Dziony, W.; Caccamo, L.; Ledig, J.; Mohajerani, M. S.; Schimpke, T.; Bähr, M.; Lilienkamp, G.; Daum, W.; Seibt, M.; Straßburg, M.; Wehmann, H.-H.; Waag, A. *Phys. status solidi* **2015**, *212* (12), 2830–2836.

https://doi.org/10.24355/dbbs.084-201912181044-0